



ELSEVIER

Available online at www.sciencedirect.com

SCIENCE @ DIRECT®

Journal of Sound and Vibration 282 (2005) 553–572

JOURNAL OF
SOUND AND
VIBRATION

www.elsevier.com/locate/jsvi

Short Communication

Vibration analysis of PWR fuel rod

Hyeong Koo Kim^{a,*}, Moon Saeng Kim^b

^a*Department of Fuel Design, KOREA Nuclear Fuel Co. Technology Center, Yuseong-Gu, Deokjin-Dong 493, Daejeon, Republic of Korea*

^b*Department of Mechanical Engineering, Pusan National University, Pusan, Republic of Korea*

Received 19 March 2003; received in revised form 28 November 2003; accepted 15 April 2004

Available online 5 November 2004

Abstract

Many reactor components including fuel assembly, heat exchanger tubes and control element assembly are typically beam-type structures with either classical or nonclassical boundary conditions, or both. In such cases, it is quite difficult to evaluate the vibration characteristics of the structures since methods for calculating accurate natural frequencies of those structures with complicated restraints are not generally available. In this study, the frequency equations for calculating the natural frequencies of the beams with generally restrained boundary conditions by both translational and rotational springs are derived in the matrix form using Fourier sine series. In order to show the validation of the solution, numerical results for two degenerate cases are compared with the existing results for natural frequency obtained by the conventional analysis. And as a specific application, the natural frequencies of fuel rod for Korean Standard Nuclear Plant (KSNP) fuel assembly are calculated and compared with the external excitations. As a result, the frequency equation derived by present paper seems to be very useful to evaluate the fuel rod vibration with various boundary conditions. Especially, when some parametric analyses are needed to modify fuel design, the equation can be applied very easily.

© 2004 Elsevier Ltd. All rights reserved.

*Corresponding author. Tel.: +1-82-42-868-1183; fax: +1-82-42-868-1149.

E-mail address: hkkim@knfc.co.kr (H.K. Kim).

1. Introduction

The fuel assembly for a typical pressurized water reactor (PWR) plant (see Fig. 3) is operated under severe operating conditions such as high temperature, high pressure and massive coolant passing through the fuel assembly with high speed. Therefore, the fuel assembly should be designed not only to sustain its structural integrity under all of the operating conditions including the most serious postulated accidents like seismic and loss of coolant accident (LOCA) events, but also to ensure that the natural frequencies of the fuel are mismatched with all of the external excitation frequencies during the operation. In general, three sources of external excitation are recognized in evaluating the fuel rod susceptibility to vibration damage. Those are reactor coolant pump blade passing frequencies, vortex shedding frequencies, and lower support structure motion. In order to prevent fuel failure due to the external excitation, fuel rods are supported by multiple spacer grids, which carefully decided the number and spacing under consideration of vibration modes, with appropriate spring forces along its length. In the fuel rod vibration, there are a number of possible combinations of neighboring span effects according to supporting conditions of the spacer grids and pellet/cladding contact effects according to progress of burn-up. Furthermore, because the vibration of the fuel rod is quite sensitive to those effects explained above, it is very difficult to evaluate the natural frequencies of the fuel rod and to verify that none of these frequencies matches the frequencies of external excitation.

For the fuel rod vibration problem, dynamic characteristics of fuel rod for PWR fuel assembly have been estimated through vibration tests with the fuel rods actual boundary conditions but analytical results of the problem have rarely been reported. However, numerous studies, which can be applicable to vibration analysis of complicated structure like fuel rod, have been carried out for various cases. The brief presented component mode method based on Fourier series for vibration of structures by using Lagrange's equations and Lagrange multipliers based on the discrete technique of component mode analysis. In the analyses, mode shapes are written in terms of Rayleigh–Ritz expansions involving simple Fourier sine or cosine series for each of the component [1,2]. Chung presented a solution method for calculating the natural frequencies and modes of beams with any of the classical boundary conditions and with unlimited intermediate supports by using Fourier series in conjunction with Lagrange multipliers. In this paper, he solved various beam problems having intermediate supports, but just considered the beams with classical boundary conditions [3]. And the applicability of Fourier series to the dynamic analysis of beams with arbitrary boundary conditions was studied by Wang [4]. He derived the frequency equation for a simply supported beam with rotational restraints at both ends by using Fourier sine series.

In this study, in order to establish a methodology which makes it possible to analyze the dynamic characteristics of the structures like nuclear fuel assembly and fuel rods including complicated factors concerned with elastic restraints, intermediate support, elastically attached masses, etc., the general frequency equation for calculating the natural frequencies of the double span beam with generally restrained boundary conditions is derived in the matrix form using Fourier series. In order to show the validation of the equation, numerical results for two degenerate cases are compared with existing results shown in literatures. And then as a specific application, a numerical analysis on the fuel rod for a typical Korean PWR fuel assembly has been performed and compared with external excitation. The results showed that none of the natural frequencies of the considered fuel rod matches with external excitation.

2. General theoretical formulations

Let us consider a uniform Bernoulli–Euler double span beam with elastically restrained boundary conditions as shown in Fig. 1. The equation of motion for free flexural vibrations of a double span uniform elastic beam ignoring shear deformation and rotary inertia effects is

$$EI \frac{\partial^4 w_i(x, t)}{\partial x_i^4} + \rho A \frac{\partial^2 w_i(x, t)}{\partial t^2} = 0 \quad (i = 1, 2), \tag{1}$$

where $w_i(x, t)$ is the lateral displacement at distance x along the length of the beam and time t , EI is the flexural rigidity of the beam, ρ is the mass density and A is the cross-sectional area of the beam.

For any mode of vibration, the lateral displacement $w_i(x, t)$ may be written in the form

$$w_i(x, t) = \psi_i(x) \cos \omega t \quad (i = 1, 2), \tag{2}$$

where $\psi_i(x)$ is modal displacement function and ω is the natural frequency. The function $\psi_i(x)$ may be written either as a Fourier sine series or cosine series. In the present study, let us consider a Fourier sine series as a mode function. Since direct differentiation of a Fourier sine series leads to a cosine series without the constant term, it is not considered to be a complete set of functions. The function is defined in two separate regions, one for boundary points and the other for the intermediate region between the boundary points as follows:

$$\psi_i(x) = \begin{cases} \psi_{i0}, & x = 0, \\ \psi_{iL}, & x = L, \\ \sum_{m=1}^{\infty} A_{im} \sin \frac{m\pi x}{L}, & 0 < x < L. \end{cases} \quad (i = 1, 2). \tag{3}$$

To obtain the correct series expressions for derivatives of a Fourier series, Stoke’s transformation must be employed. Stoke’s transformation consists of defining each derivative with an independent series and integrating the newly defined series by parts to obtain the relationship between the Fourier coefficients [2–4].

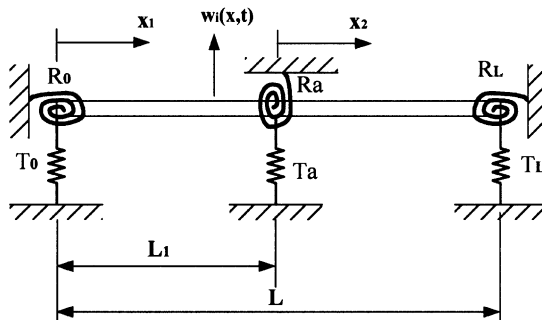


Fig. 1. An elastic double span Bernoulli–Euler beam with rotational and translational restraints.

The derivatives of $\psi_i(x)$ based on the usual definitions of Fourier series become

$$\frac{d\psi_i(x)}{dx} = \frac{\psi_{iL} - \psi_{i0}}{L} + \sum_{m=1}^{\infty} \left[\frac{2}{L} \{ \psi_{iL}(-1)^m - \psi_{i0} \} + \alpha_m A_m \right] \cos \alpha_m x, \quad 0 \leq x \leq L, \tag{4}$$

where $\alpha_m = m\pi/L$ and subscript $i = 1, 2$.

$$\frac{d^2\psi_i(x)}{dx^2} = - \sum_{m=1}^{\infty} \alpha_m \left[\frac{2}{L} \{ \psi_{iL}(-1)^m - \psi_{i0} \} + \alpha_m A_m \right] \sin \alpha_m x, \quad 0 < x < L, \tag{5}$$

$$\psi''_{i0} = \psi''_i(0), \quad \psi''_{iL} = \psi''_i(L),$$

$$\begin{aligned} \frac{d^3\psi_i(x)}{dx^3} = & \frac{\psi''_{iL} - \psi''_{i0}}{L} + \sum_{m=1}^{\infty} \left[\frac{2}{L} \{ \psi''_{iL}(-1)^m - \psi''_{i0} \} - \alpha_m^2 \left(\frac{2}{L} \{ \psi_{iL}(-1)^m - \psi_{i0} \} + \alpha_m A_m \right) \right] \\ & \times \cos \alpha_m x, \quad 0 \leq x \leq L \end{aligned} \tag{6}$$

and

$$\begin{aligned} \frac{d^4\psi_i(x)}{dx^4} = & - \sum_{m=1}^{\infty} \alpha_m \left[\frac{2}{L} \{ \psi''_{iL}(-1)^m - \psi''_{i0} \} - \alpha_m^2 \left(\frac{2}{L} \{ \psi_{iL}(-1)^m - \psi_{i0} \} + \alpha_m A_m \right) \right] \\ & \times \sin \alpha_m x, \quad 0 < x < L. \end{aligned} \tag{7}$$

The function can also be represented by Fourier cosine series in a similar manner.

In order to obtain a general expression for the flexure of beams, let us substitute Eqs. (5) and (7) into Eq. (1). Then, we can get the displacement function for the free vibration of double span beam having no geometrical constraints at both ends as follows:

$$\begin{aligned} w_i(x, t) = & \sum_{m=1}^{\infty} \frac{2}{\alpha_m^3 L} \frac{\omega_n^2}{\omega^2 - \omega_n^2} \{ (\psi''_i(0) - (-1)^m \psi''_i(L)) - \alpha_m^2 (\psi_i(0) - (-1)^m \psi_i(L)) \} \\ & \times \sin \alpha_m x \cos \omega t \quad (i = 1, 2), \end{aligned} \tag{8}$$

where

$$A_{im} = \sum_{m=1}^{\infty} \frac{2}{\alpha_m^3 L} \frac{\omega_n^2}{\omega^2 - \omega_n^2} \{ (\psi''_0 - (-1)^m \psi''_L) - \alpha_m^2 (\psi_0 - (-1)^m \psi_L) \}, \quad \omega_n^2 = \frac{EI}{\rho A} \alpha_m^4. \tag{9}$$

The elastically restrained boundary conditions of the beam shown in Fig. 1 are as follows:

$$T_0 w_1(0) = -EI \frac{\partial^3 w_1(0)}{\partial x^3}, \quad R_0 \frac{\partial w_1(0)}{\partial x} = EI \frac{\partial^2 w_1(0)}{\partial x^2} \quad \text{at } x_1 = 0, \tag{10,11}$$

$$T_L w_2(L) = EI \frac{\partial^3 w_2(L)}{\partial x^3}, \quad R_L \frac{\partial w_2(L)}{\partial x} = -EI \frac{\partial^2 w_2(L)}{\partial x^2} \quad \text{at } x_2 = L, \tag{12,13}$$

$$w_1(L_1) = w_2(L_1), \quad \frac{\partial w_1(L_1)}{\partial x} = \frac{\partial w_2(L_1)}{\partial x} \quad \text{at } x_1 = L_1, \tag{14,15}$$

$$\begin{aligned}
 EI \frac{\partial^2 w_1(L_1)}{\partial x^2} &= R_a \frac{\partial w_1(L_1)}{\partial x} + EI \frac{\partial^2 w_2(L_1)}{\partial x^2}, \\
 EI \frac{\partial^3 w_1(L_1)}{\partial x^3} &= T_a w_1(L_1) + EI \frac{\partial^3 w_2(L_1)}{\partial x^3} \quad \text{at } x_1 = L_1
 \end{aligned}
 \tag{16, 17}$$

in which T_0 , T_a and T_L are translational spring constants, and R_0 , R_a and R_L are rotational spring constants at $x_1 = 0, L_1$ and L , respectively. Substitution of Eq. (3) and its derivatives into Eqs. (10)–(17) leads to the homogeneous matrix equation

$$[SS_{ij}]\{\psi''_{10}, \psi''_{1L}, \psi_{10}/L^2, \psi_{1L}/L^2, \psi''_{20}, \psi''_{2L}, \psi_{20}/L^2, \psi_{2L}/L^2\}^T = \{0\} \quad (i, j = 1, 2, 3, 4, 5, 6, 7, 8). \tag{18}$$

For nontrivial solution the determinant of the coefficient matrix of Eq. (18) must vanish, i.e.

$$|SS_{ij}| = 0 \quad (i, j = 1, 2, 3, 4). \tag{19}$$

From the determinant, frequency equation of an elastic double span Bernoulli–Euler beam with rotational and translational restraints is obtained. Each element of the SS determinant is shown in Appendix A.

3. Degenerate case

A typical degenerate case is considered to show that the determinant derived in this study can be applied to classical boundary conditions and nonclassical boundary conditions can be restrained by general springs.

3.1. Single span beam with translational and rotational spring restraints at both ends

In this case, since there is no intermediate support, the boundary conditions can be written with Eqs. (10)–(13). The frequency equation for this case can be easily given from the frequency equation for double span beam by deleting columns and rows for the intermediate support. Then the resultant frequency equation is given as

$$|S_{ij}| = \begin{vmatrix} SS_{11} & SS_{12} & SS_{13} & SS_{14} \\ SS_{21} & SS_{22} & SS_{23} & SS_{24} \\ SS_{35} & SS_{36} & SS_{37} & SS_{38} \\ SS_{45} & SS_{46} & SS_{47} & SS_{48} \end{vmatrix} = 0 \quad (i, j = 1, 2, 3, 4). \tag{20}$$

3.2. CC beam with an intermediate translational spring restraint

For a CC (clamped–clamped) beam with an intermediate translational spring restraint as shown in Fig. 2, the resulting boundary conditions are

$$w_1(L_1) = w_2(L_1), \quad \frac{\partial w_1(L_1)}{\partial x} = \frac{\partial w_2(L_1)}{\partial x} \quad \text{at } x_1 = L_1,$$

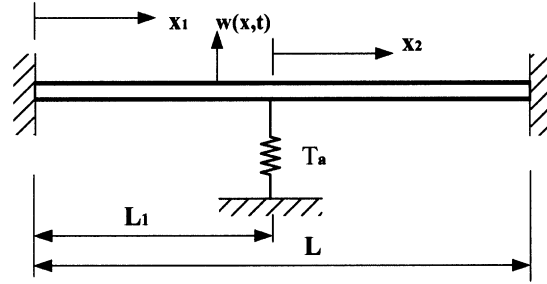


Fig. 2. CC beam with an intermediate translational spring restraint.

$$\frac{\partial^2 w_1(L_1)}{\partial x^2} = \frac{\partial^2 w_2(L_1)}{\partial x^2}, \quad EI \frac{\partial^3 w_1(L_1)}{\partial x^3} = T_a w_1(L_1) + EI \frac{\partial^3 w_2(L_1)}{\partial x^3} \quad \text{at } x_1 = L_1,$$

$$w_1(0) = 0, \quad \frac{\partial w_1(0)}{\partial x} = 0 \quad \text{at } x_1 = 0,$$

$$w_2(L) = 0, \quad \frac{\partial w_2(L)}{\partial x} = 0 \quad \text{at } x_2 = L. \quad (21)$$

Substitution of Eq. (3) and its derivatives into Eq. (15) leads to the eight simultaneous homogeneous equations as follows:

$$[\text{CTC}_{ij}] \{\psi''_{10}, \psi''_{1L}, \psi_{10}/L^2, \psi_{1L}/L^2, \psi''_{20}, \psi''_{2L}, \psi_{20}/L^2, \psi_{2L}/L^2\}^T = \{0\} \quad (i, j = 1, 2, 3, 4, 5, 6, 7, 8). \quad (22)$$

In order to have nontrivial solution, the determinant of the coefficient matrix must vanish, i.e.

$$|\text{CTC}_{ij}| = 0 \quad (i, j = 1, 2, 3, 4, 5, 6, 7, 8). \quad (23)$$

Or theoretically we can get same result from Eq. (19) by just putting $\bar{T}_0, \bar{R}_0 \rightarrow \infty, \bar{R}_a \rightarrow 0$ and $\bar{T}_L, \bar{R}_L \rightarrow \infty$ instead of Eq. (23). The elements of this CTC determinant are shown in Appendix B.

4. Frequency equations of PWR fuel rod

4.1. Description of PWR fuel rod

The fuel rods consist of slightly enriched UO_2 cylindrical ceramic pellets, a round wire Type 302 stainless-steel compression spring, and an alumina spacer disc located at the lower end of the fuel column, all encapsulated within a Zircaloy-4 cladding tube seal welded with Zircaloy-4 end caps as shown in Fig. 3. The fuel rods are supported by 11 spacer grids along the length. The number and spacing of grids must ensure that the natural frequencies of unsupported lengths of fuel rods are significantly mismatched with the expected excitation frequencies. Three sources of external excitation are recognized in evaluating the fuel rod susceptibility to vibration damage. These sources are as follows:

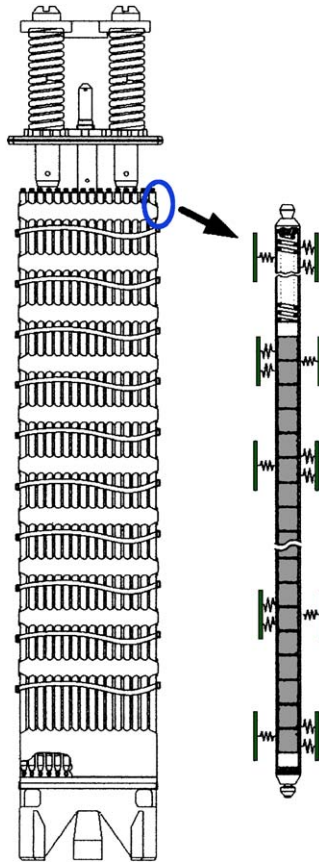


Fig. 3. KSNP fuel assembly.

Reactor coolant pump blade passing frequencies: Comprehensive vibration assessment programs on Korean Standard Nuclear Plant (KSNP) reactors indicate that peak pressure pulses are expected at the pump blade passing frequency.

Vortex shedding frequencies: The vortex shedding frequencies at the various elevation of the fuel assembly are listed in Table 1 [5].

Lower support structure motion: Random lateral motion between the fuel assembly and the lower support structure is expected to occur with an amplitude in the some frequency ranges.

Because there are a number of possible combinations of neighboring span effects according to pellet/cladding contact effects and supporting conditions, the natural frequency of fuel rod should be investigated to cover a number of possible modes. And then it should be verified that none of these frequencies matches the frequencies of external excitation. There are three possible contact configurations between pellet and cladding as follows:

Case A. No contact: This configuration applies for all rods at the beginning-of-life (BOL) and throughout fuel life in the plenum region. The frequency of fuel rod vibration depends on that of

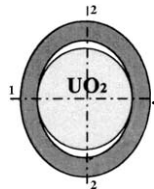
Table 1
Typical normalized external excitation frequencies of a KSNP reactor

External excitation sources	Normalized frequencies
Reactor coolant pump blade passing frequencies	10,20,60,120, 180,240
<i>Vortex shedding</i>	
Uppermost rod end	
Top grid span	1.5,7
Intermediate grid span	
Lower grid span	1.5,3.5,4,7,12
Lowermost end	8.5,9.5,18,20,63.5,71
Lower support structure motion	1,2,3,4,5

cladding alone.



Case B. Line contact: This configuration occurs after temperature and pressure effects have caused the cladding to contact the pellets in an oval configuration. Since there is no complete contact between pellets and cladding, pellets are not assumed to contribute to rod stiffness. However, the mass of the pellet is assumed to be carried by the rod in lateral vibration and is thus included in the calculated frequency.



Case C. Hard contact: Late in fuel life, except in low fluence regions, the pellets have expanded due to irradiation, to the point where they contribute both to their mass and rigidity to a vibrating rod.



The fuel rods are restrained from axial and lateral motions by the forces of the spacer grid leaf springs and arches being located 11 points along the length of fuel rod as shown in Fig. 3.

4.2. Frequency equations of fuel rod

To investigate the integrity of fuel rod under external excitation loads, natural frequencies for all feasible combinations of vibration modes and pellet to cladding contact configurations explained previous section should be calculated. The applicable vibration modes to fuel rod are shown in Table 2. All of the vibration modes can be expressed easily by the frequency equation being derived in previous section, as follows:

For Mode I:

$$|SS_{ij}| = 0 \quad (i, j = 1, 2, 3, 4, 5, 6, 7, 8), \text{ where } \bar{R}_0 = \bar{R}_a = \bar{R}_L = 0 \text{ and } \bar{T}_0 = \bar{T}_a = \bar{T}_L = \infty.$$

For Mode II:

$$|S_{ij}| = 0 \quad (i, j = 1, 2, 3, 4), \text{ where } \bar{T}_0 = \bar{T}_L = \infty \text{ and } \bar{R}_0 = \bar{R}_L = 0.$$

For Mode III:

$$|S_{ij}| = 0 \quad (i, j = 1, 2, 3, 4), \text{ where } \bar{R}_0 = 0 \text{ and } \bar{R}_L = 0.$$

For Modes IV and VII, the lumped mass effect can be implemented by replacing \bar{T}_L with $-\bar{M}\Omega$ as Eq. (24).

$$\begin{vmatrix} \left(1 + 2 \sum_{m=1}^{\infty} \frac{(-1)^m \Omega}{\Omega - m^4}\right) & \left(-\bar{M}(\pi^4 \Omega) + 2\pi^2 \sum_{m=1}^{\infty} \frac{m^2 \Omega}{\Omega - m^4}\right) \\ \left(1 - \frac{2\bar{R}_0}{\pi^2} \sum_{m=1}^{\infty} \frac{m^2}{\Omega - m^4}\right) & -\left(\bar{R}_0 + 2\bar{R}_0 \sum_{m=1}^{\infty} \frac{(-1)^m \Omega}{\Omega - m^4}\right) \end{vmatrix} = 0, \quad (24)$$

where $\bar{M} = M(\rho AL)$.

Here the modes for Modes IV and VII can be obtained from Eq. (19) by letting $\bar{R}_0 = 0$ and $\bar{R}_0 = \infty$, respectively.

For mode V, the frequency equations are shown in the previous degenerate case.

$$|CTC_{ij}| = 0, \quad (i, j = 1, 2, 3, 4, 5, 6, 7, 8).$$

For Mode VI:

$$|S_{ij}| = 0, \quad (i, j = 1, 2, 3, 4) \text{ where } \bar{T}_0 = \bar{T}_L = \infty \text{ and } \bar{R}_0 = \bar{R}_L = \infty.$$

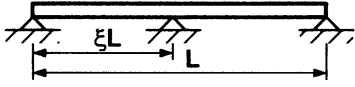
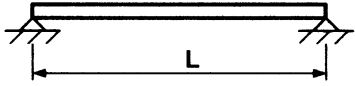
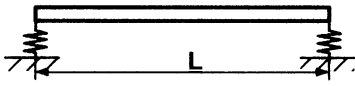
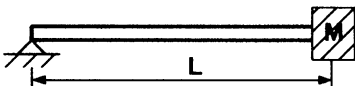

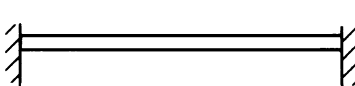
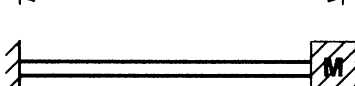
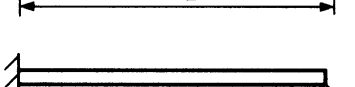
For Mode VIII:

$$|S_{ij}| = 0, \quad (i, j = 1, 2, 3, 4) \text{ where } \bar{R}_0 = \infty, \bar{K}_0 = \infty, \bar{K}_L = \infty \text{ and } \bar{R}_L = 0.$$

The fuel rod can be divided into five parts according to its properties as follows:

- *Uppermost rod end:* Upper end of fuel rod would be vibrating per Modes A-IV and A-VII.
- *Top grid span:* Because the top span consists mostly of plenum region and a low fluence pellet region, pellet interaction effects with cladding are not considered. Fuel rods would be vibrating under Modes A-II, A-III and A-VIII.

Table 2
Vibration modes of fuel rod

Case	Mode	Application
I		Intermediate grid span Lower grid span
II		Top grid span Intermediate grid span Lower grid span
III		Top grid span Intermediate grid span Lower grid span
IV		Uppermost rod end Lowermost rod end
V		Intermediate grid span Lower grid span
VI		Top grid span Intermediate grid span Lower grid span
VII		Lowermost rod end
VIII		Top grid span Lower grid span

- *Intermediate grid spans*: These spans are uniform in cross section, but would be vibrating together or independently due to different rates of pellet swelling, grid relaxation or cross flow of reactor coolant. Thus pellet/cladding configurations A, B or C can combine with vibration Modes I–VI.
- *Lower grid span*: The lower span would be vibrating under Modes I–VIII. And the pellet/cladding configurations A, B or C should be combined with the modes.
- *Lowermost rod end*: As in the case of the uppermost end, the lower end span would be vibrating under Modes VII because of its high constraint condition. In addition, because of the lower fluences in the lower end of the rods, no hard contact is considered.

5. Numerical analysis

Numerical investigation has been performed to confirm the validity of the present formulation for an elastic double span Bernoulli–Euler beam with rotational and translational restraints as well as typical classical boundary conditions. However, in this paper, the results on the two degenerate cases are represented as follows.

5.1. CC beam with an intermediate translational spring restraint

The eigenvalues of the CC (clamped–clamped) beam with an intermediate translational spring restraint as shown in Fig. 3 are provided in Table 3. And Fig. 4 shows the two- and three-dimensional plots of the Table 3. Fig. 4 shows very good agreement with Fig. 2 of Ref. [6] which is an analytical solution from the frequency equation derived by solving the governing equation exactly and invoking boundary conditions and continuity conditions. Fig. 5 shows a typical plot of the frequency parameter for the CC beam with an intermediate translational spring restraint. The sensitivity of the terms in this problem has been investigated for the case of $\xi = 0.1$, $\bar{T}_a = 100$. Fig. 6 shows the sensitivity of the number of terms in the series. It has been shown that the first 50 terms will be enough to get the desirable accuracy. But, the values of Table 3 have been obtained using the first 100 terms of the infinite series based on the result of the sensitivity study which bring a converged value at 100 terms. As shown in Fig. 4, the dimensionless translational spring parameter \bar{T}_a is highly transcendental in nature and the effect of increasing the parameter \bar{T}_a is to increase the frequency parameter β . And it is interesting to notice the fact that when the parameter \bar{T}_a reaches 2E3, the natural frequencies of the beam reach a nearly saturated value. All of these calculations have been performed with Mathematica.

Table 3
The 1st natural frequency parameter (β) for CC beam with an intermediate translational spring restraint

\bar{T}_a	ξ										
	0	0.1	0.2	0.3	0.4	0.5	0.6	0.7	0.8	0.9	1
0	4.74948	4.74948	4.74948	4.74948	4.74948	4.74948	4.74948	4.74948	4.74948	4.74948	4.74948
10	4.74948	4.75034	4.75845	4.77721	4.79816	4.80738	4.79816	4.77721	4.75845	4.75034	4.74948
100	4.74948	4.75793	4.83169	4.99012	5.16452	5.24382	5.16452	4.99012	4.83169	4.75793	4.74948
200	4.74948	4.76593	4.89988	5.16918	5.46753	5.61137	5.46753	5.16918	4.89988	4.76593	4.74948
300	4.74948	4.77351	4.96716	5.30738	5.70093	5.90437	5.70093	5.30738	4.96716	4.77351	4.74948
400	4.74948	4.78070	5.00602	5.41689	5.88627	6.14732	5.88627	5.41689	5.00602	4.78070	4.74948
500	4.74948	4.78753	5.04809	5.50549	6.03635	6.35410	6.03635	5.50549	5.04809	4.78753	4.74948
1E3	4.74948	4.81710	5.19290	5.77295	6.48201	7.06854	6.48201	5.77295	5.19290	4.81710	4.74948
1.5E3	4.74948	4.84071	5.27740	5.90444	6.68662	7.50056	6.68662	5.90444	5.27740	4.84071	4.74948
2E3	4.74948	4.85997	5.33249	5.98138	6.79740	7.79601	6.79740	5.98138	5.33249	4.85997	4.74948
5E3	4.74948	4.92727	5.46491	6.14124	6.99890	7.88459	6.99890	6.14124	5.46491	4.92727	4.74948
1E4	4.74948	4.97212	5.52220	6.20080	7.06311	7.88535	7.06311	6.20080	5.52220	4.97212	4.74948
1E6	4.74948	5.04517	5.58756	6.26269	7.12366	7.88535	7.12366	6.26269	5.58756	5.04517	4.74948
1E8	4.74948	5.04613	5.58826	6.26332	7.12425	7.88535	7.12425	6.26332	5.58826	5.04613	4.74948

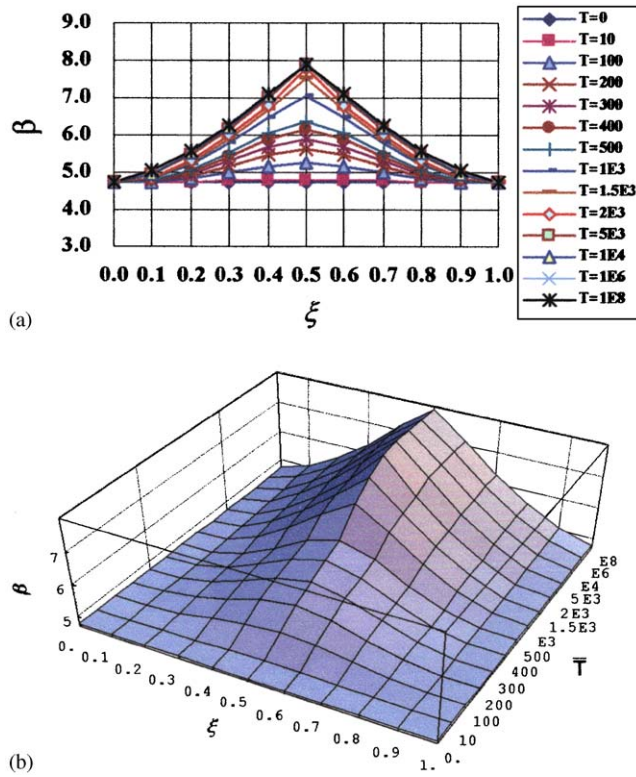


Fig. 4. The fundamental frequency parameter of the CC beam with an intermediate translational spring restraint: (a) two dimensional; (b) three dimensional.

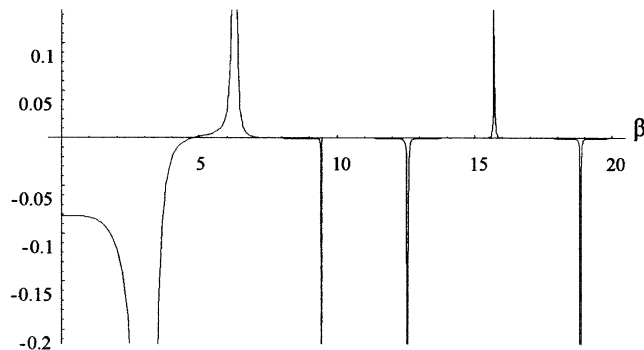


Fig. 5. The plot of frequency parameter for the CC beam with an intermediate restraint.

Besides, the cases presented the results in this paper, the various degenerate cases have been investigated and showed good agreement with the previous results [7,8]. The results were shown in the author's previous paper [9].

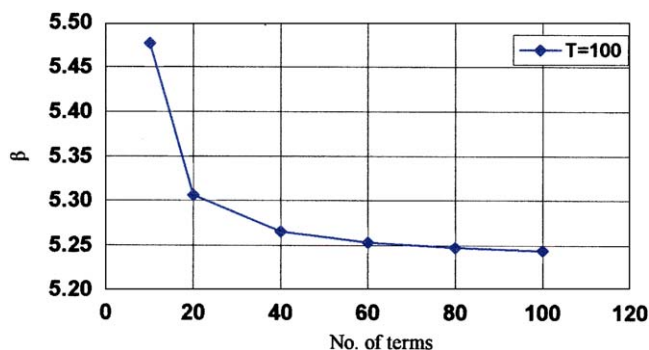


Fig. 6. The sensitivity of the number of terms.

5.2. A PWR fuel rod with various vibration modes

Using the frequency equations explained in previous sections, the natural frequencies of each fuel rod span have been evaluated and provided in Table 4. The natural frequency of a fuel rod span changes as a function of time in core, for example, the normalized natural frequency in Case A-I & II at an intermediate span, which means the condition at BOL, $\bar{f}_n = 45$, after a time in core and because some ovality exists $\bar{f}_n = 21.85$ or 21.5 and after fuel pellets have completely swollen such that hard contact results $\bar{f}_n = 46.5$. Parameters such as cladding tolerance, strip thickness of grids, time in life and fixity have a measurable effect on a span's natural frequency.

The hydraulic induced vibration, vortex shedding would not produce fretting in the cladding from contact with spacer grids because at the lower rod end normalized vortex shedding frequency is 63.5 to 71 where normalized rod frequencies are 217.45, 221.15 or 330.8.

As can be seen in Tables 1 and 4, most of the normalized natural frequencies do not match with sources frequencies except some frequencies, e.g., 20.6, 21 or 21.5 vs. 20 normalized pump blade passing frequency. However, in this calculation damping factors, which can be observed in the fuel assembly structural tests, are not considered, so the actual magnification factor should be small.

It is very difficult and tedious to analyze the dynamic characteristics of beams with various vibration modes including the nonclassical boundary conditions as well as the change of the mechanical characteristics of the structure like fuel rod. However, the frequency equation derived in present paper can be easily applicable to those structures by simply introducing the boundary conditions of the structure to the equations, as shown in numerical analysis on the fuel rod vibration. And as the equation has been derived using Fourier series, it is also very easy to control the accuracy of the solutions by controlling the number of terms.

6. Conclusions

The frequency expressions for double span Bernoulli–Euler beams with generally restrained boundary conditions have been presented by using Fourier series as a mode function. The expressions are quite general since identical Fourier series expressions may be used for many

Table 4

Calculated fuel rod frequency parameters and corresponding normalized natural frequencies

Fuel rod span	Modes	Frequency parameter β	Normalized natural frequencies
Uppermost rod end	A-IV	3.3507	4273.90
	A-VII	1.3977	743.65
Top grid span	A-II	π	45.00
	A-III	3.07692	43.15
Intermediate grid span	A-VIII	3.92819	70.35
	A-I & II	π	45.00
	B1-I & II	π	21.85
	B2-I & II	π	21.50
	C-I & II	π	46.50
	A-III	3.07692	43.15
	B1-III	3.07692	21.00
	B2-III	3.07692	20.60
	C-III	2.87232	39.00
	A-V	7.88520	70.85
	B1-V	7.88520	34.45
	B2-V	7.88520	33.35
	C-V	7.88520	73.45
	A-VI	4.73004	102.00
B1-VI	4.73004	49.50	
B2-VI	4.73004	48.70	
C-VI	4.73004	105.60	
Lower grid span	A-I	6.26651	49.00
	B1-I	6.26651	23.85
	B2-I	6.26651	23.45
	C-I	6.26651	50.80
	A-II	π	54.25
	B1-II	π	26.40
	B2-II	π	25.95
	C-II	π	56.25
	A-III	3.05943	51.50
	B1-III	3.05943	25.00
	B2-III	3.06200	24.65
	C-III	2.80812	44.95
	A-V	7.60887	72.30
	B1-V	7.60887	35.15
	B2-V	7.60887	34.55
	C-V	7.60887	74.95
	A-VI	4.73004	123.00
	B1-VI	4.73004	59.80
	B2-VI	4.73004	58.80
	C-VI	4.73004	127.50
A-VIII	3.92819	84.85	
B1-VIII	3.92819	41.25	
B2-VIII	3.92819	40.55	
C-VIII	3.92819	87.95	
Lowermost rod end	A-VII	1.48283	330.80
	B1-VII	1.73904	221.15
	B2-VII	1.73904	217.45

A: No contact; B1: Line contact (based on minor axis); B2: Line contact (based on major axis); C: Hard contact.

different physical problems like beams, columns, strings, plates and shells with both classical and nonclassical boundary conditions.

The hydraulic-induced vibration, vortex shedding would not produce fretting in the KSNP fuel rods because at the lower rod end normalized vortex shedding frequency is 63.5–71 where normalized rod frequencies are 217.45, 221.15 or 330.8.

The frequency equations derived in the present paper have been successfully applied to the design analysis of fuel rod. As a result, therefore, the frequency equation derived by the present paper seems to be very useful to evaluate the fuel rod vibration with various boundary conditions. Especially, when some parametric analyses are needed to modify fuel design, the equation can be a very easy and useful tool.

Appendix A. Components of matrix |SS_{ij}|

$$\begin{aligned}
 SS_{11} &= -\left(1 + 2 \sum_{m=1}^{\infty} \frac{\Omega}{\Omega - m^4}\right), & SS_{12} &= \left(1 + 2 \sum_{m=1}^{\infty} \frac{(-1)^m \Omega}{\Omega - m^4}\right), \\
 SS_{13} &= \left(\bar{T}_0 + 2\pi^2 \sum_{m=1}^{\infty} \frac{m^2 \Omega}{\Omega - m^4}\right), & SS_{14} &= -\left(2\pi^2 \sum_{m=1}^{\infty} \frac{(-1)^m m^2 \Omega}{\Omega - m^4}\right), \\
 SS_{15} &= SS_{16} = SS_{17} = SS_{18} = 0, \\
 SS_{21} &= \left(1 - \frac{2\bar{R}_0}{\pi^2} \sum_{m=1}^{\infty} \frac{m^2}{\Omega - m^4}\right), & SS_{22} &= \left(\frac{2\bar{R}_0}{\pi^2} \sum_{m=1}^{\infty} \frac{(-1)^m m^2}{\Omega - m^4}\right), \\
 SS_{23} &= \bar{R}_0 SS_{36}, & SS_{24} &= -\bar{R}_0 SS_{12}, & SS_{25} &= SS_{26} = SS_{27} = SS_{28} = 0, \\
 SS_{31} &= SS_{32} = SS_{33} = SS_{34} = 0, & SS_{35} &= SS_{12}, & SS_{36} &= -SS_{11}, & SS_{37} &= SS_{14}, \\
 SS_{38} &= \left(\bar{T}_L + 2\pi^2 \sum_{m=1}^{\infty} \frac{m^2 \Omega}{\Omega - m^4}\right), \\
 SS_{41} &= SS_{42} = SS_{43} = SS_{44} = 0, & SS_{45} &= \left(\frac{2\bar{R}_L}{\pi^2} \sum_{m=1}^{\infty} \frac{(-1)^m m^2}{\Omega - m^4}\right), \\
 SS_{46} &= \left(1 - \frac{2\bar{R}_L}{\pi^2} \sum_{m=1}^{\infty} \frac{m^2}{\Omega - m^4}\right), & SS_{47} &= -\bar{R}_L SS_{12}, & SS_{48} &= \bar{R}_L SS_{11}, \\
 SS_{51} &= \sum_{m=1}^{\infty} \left(\frac{m \sin(m\pi\xi_1)}{\pi^2(\Omega - m^4)}\right), & SS_{52} &= -\sum_{m=1}^{\infty} \left(\frac{(-1)^m m \sin(m\pi\xi_1)}{\pi^2(\Omega - m^4)}\right),
 \end{aligned}$$

$$\begin{aligned}
SS_{53} &= -\sum_{m=1}^{\infty} \left(\frac{m^3 \sin(m\pi\xi_1)}{(\Omega - m^4)} \right), & SS_{54} &= \sum_{m=1}^{\infty} \left(\frac{(-1)^m m^3 \sin(m\pi\xi_1)}{(\Omega - m^4)} \right), \\
SS_{55} &= -SS_{51}, & SS_{56} &= -SS_{52}, & SS_{57} &= -SS_{53}, & SS_{58} &= -SS_{54}, \\
SS_{61} &= \sum_{m=1}^{\infty} \left(\frac{2m^2 \cos(m\pi\xi_1)}{\pi^2(\Omega - m^4)} \right), & SS_{62} &= -\sum_{m=1}^{\infty} \left(\frac{2(-1)^m m^2 \cos(m\pi\xi_1)}{\pi^2(\Omega - m^4)} \right), \\
SS_{63} &= -\left(1 + \sum_{m=1}^{\infty} \frac{2\Omega \cos(m\pi\xi_1)}{(\Omega - m^4)} \right), & SS_{64} &= \left(1 + \sum_{m=1}^{\infty} \frac{2(-1)^m \Omega \cos(m\pi\xi_1)}{(\Omega - m^4)} \right), \\
SS_{65} &= -SS_{61}, & SS_{66} &= -SS_{62}, & SS_{67} &= -SS_{63}, & SS_{68} &= -SS_{64}, \\
SS_{71} &= \left(\sum_{m=1}^{\infty} \frac{2\bar{R}_a m^2 \cos(m\pi\xi_1)}{\pi^2(\Omega - m^4)} - SS_{75} \right), & SS_{72} &= -(\bar{R}_a SS_{66} + SS_{76}), \\
SS_{73} &= -(\bar{R}_a SS_{67} + SS_{77}), & SS_{74} &= (\bar{R}_a SS_{64} - SS_{78}), \\
SS_{75} &= \sum_{m=1}^{\infty} \left(\frac{2m^3 \sin(m\pi\xi_1)}{\pi(\Omega - m^4)} \right), & SS_{76} &= -\sum_{m=1}^{\infty} \left(\frac{2(-1)^m m^3 \sin(m\pi\xi_1)}{\pi(\Omega - m^4)} \right), \\
SS_{77} &= -\sum_{m=1}^{\infty} \left(\frac{2m\pi\Omega \sin(m\pi\xi_1)}{(\Omega - m^4)} \right), & SS_{78} &= \sum_{m=1}^{\infty} \left(\frac{2(-1)^m m\pi\Omega \sin(m\pi\xi_1)}{(\Omega - m^4)} \right), \\
SS_{81} &= SS_{85} - \sum_{m=1}^{\infty} \left(\frac{2\bar{T}_a m \sin(m\pi\xi_1)}{\pi^3(\Omega - m^4)} \right), & SS_{82} &= \left(SS_{86} + \sum_{m=1}^{\infty} \frac{2\bar{T}_a (-1)^m m \sin(m\pi\xi_1)}{\pi^3(\Omega - m^4)} \right) \\
SS_{83} &= \left(\Omega SS_{87} + \sum_{m=1}^{\infty} \left(\frac{2\bar{T}_a m^3 \sin(m\pi\xi_1)}{\pi(\Omega - m^4)} \right) \right), \\
SS_{84} &= \Omega SS_{88} - \sum_{m=1}^{\infty} \frac{2\bar{T}_a (-1)^m m^3 \sin(m\pi\xi_1)}{\pi(\Omega - m^4)}, & SS_{85} &= -\left(1 + \sum_{m=1}^{\infty} \frac{2\Omega \cos(m\pi\xi_1)}{(\Omega - m^4)} \right), \\
SS_{86} &= \left(1 + \sum_{m=1}^{\infty} \frac{2(-1)^m \Omega \cos(m\pi\xi_1)}{(\Omega - m^4)} \right), & SS_{87} &= \sum_{m=1}^{\infty} \left(\frac{2\pi^2 m^2 \cos(m\pi\xi_1)}{(\Omega - m^4)} \right), \\
SS_{88} &= -\sum_{m=1}^{\infty} \left(\frac{2\pi^2 (-1)^m m^2 \cos(m\pi\xi_1)}{(\Omega - m^4)} \right),
\end{aligned}$$

$$\text{where } \bar{T}_0 = \frac{T_0 L^3}{EI}, \quad \bar{T}_a = \frac{T_a L^3}{EI}, \quad \bar{T}_L = \frac{T_L L^3}{EI}, \quad \bar{R}_0 = \frac{R_0 L}{EI},$$

$$\bar{R}_a = \frac{R_a L}{EI}, \quad \bar{R}_L = \frac{R_L L}{EI}, \quad \omega_n^2 = \frac{EI}{\rho A} \left(\frac{m\pi}{L} \right)^4, \quad \Omega = \frac{\rho A L^4}{\pi^4 EI} \omega^2 = \frac{\beta^4}{\pi^4}.$$

Appendix B. Components of matrix $|\text{CTC}_{ij}|$

$$\begin{aligned} \text{CTC}_{11} &= 2 \sum_{m=1}^{\infty} \frac{m^3 \pi^3}{m^4 \pi^4 - \beta^4} \sin \frac{m\pi L_1}{L}, & \text{CTC}_{12} &= -2 \sum_{m=1}^{\infty} \frac{m\pi}{m^4 \pi^4 - \beta^4} \sin \frac{m\pi L_1}{L}, \\ \text{CTC}_{13} &= -2 \sum_{m=1}^{\infty} \frac{(-1)^m m^3 \pi^3}{m^4 \pi^4 - \beta^4} \sin \frac{m\pi L_1}{L}, & \text{CTC}_{14} &= 2 \sum_{m=1}^{\infty} \frac{(-1)^m m\pi}{m^4 \pi^4 - \beta^4} \sin \frac{m\pi L_1}{L}, \\ \text{CTC}_{15} &= -2 \sum_{m=1}^{\infty} \frac{m^3 \pi^3}{m^4 \pi^4 - \beta^4} \sin \frac{m\pi L_1}{L}, & \text{CTC}_{16} &= 2 \sum_{m=1}^{\infty} \frac{m\pi}{m^4 \pi^4 - \beta^4} \sin \frac{m\pi L_1}{L}, \\ \text{CTC}_{17} &= 2 \sum_{m=1}^{\infty} \frac{(-1)^m m^3 \pi^3}{m^4 \pi^4 - \beta^4} \sin \frac{m\pi L_1}{L}, & \text{CTC}_{18} &= -2 \sum_{m=1}^{\infty} \frac{(-1)^m m\pi}{m^4 \pi^4 - \beta^4} \sin \frac{m\pi L_1}{L}, \\ \text{CTC}_{21} &= - \left(1 + 2 \sum_{m=1}^{\infty} \left(1 - \frac{m^4 \pi^4}{m^4 \pi^4 - \beta^4} \right) \cos \frac{m\pi L_1}{L} \right), \\ \text{CTC}_{22} &= -2 \sum_{m=1}^{\infty} \frac{m^2 \pi^2}{m^4 \pi^4 - \beta^4} \cos \frac{m\pi L_1}{L}, \\ \text{CTC}_{23} &= \left(1 + 2 \sum_{m=1}^{\infty} \left(1 - \frac{m^4 \pi^4}{m^4 \pi^4 - \beta^4} \right) (-1)^m \cos \frac{m\pi L_1}{L} \right), \\ \text{CTC}_{24} &= 2 \sum_{m=1}^{\infty} \frac{(-1)^m m^2 \pi^2}{m^4 \pi^4 - \beta^4} \cos \frac{m\pi L_1}{L}, \\ \text{CTC}_{25} &= \left(1 + 2 \sum_{m=1}^{\infty} \left(1 - \frac{m^4 \pi^4}{m^4 \pi^4 - \beta^4} \right) \cos \frac{m\pi L_1}{L} \right), \\ \text{CTC}_{26} &= 2 \sum_{m=1}^{\infty} \frac{m^2 \pi^2}{m^4 \pi^4 - \beta^4} \cos \frac{m\pi L_1}{L}, \\ \text{CTC}_{27} &= - \left(1 + 2 \sum_{m=1}^{\infty} \left(1 - \frac{m^4 \pi^4}{m^4 \pi^4 - \beta^4} \right) (-1)^m \cos \frac{m\pi L_1}{L} \right), \end{aligned}$$

$$\begin{aligned}
\text{CTC}_{28} &= -2 \sum_{m=1}^{\infty} \frac{(-1)^m m^2 \pi^2}{m^4 \pi^4 - \beta^4} \cos \frac{m\pi L_1}{L}, \\
\text{CTC}_{31} &= 2 \sum_{m=1}^{\infty} \left(1 - \frac{m^4 \pi^4}{m^4 \pi^4 - \beta^4}\right) m\pi \sin \frac{m\pi L_1}{L}, \\
\text{CTC}_{32} &= 2 \sum_{m=1}^{\infty} \frac{m^3 \pi^3}{m^4 \pi^4 - \beta^4} \sin \frac{m\pi L_1}{L}, \\
\text{CTC}_{33} &= -2 \sum_{m=1}^{\infty} (-1)^m \left(1 - \frac{m^4 \pi^4}{m^4 \pi^4 - \beta^4}\right) m\pi \sin \frac{m\pi L_1}{L}, \\
\text{CTC}_{34} &= -2 \sum_{m=1}^{\infty} \frac{(-1)^m m^3 \pi^3}{m^4 \pi^4 - \beta^4} \sin \frac{m\pi L_1}{L}, \\
\text{CTC}_{35} &= -2 \sum_{m=1}^{\infty} \left(1 - \frac{m^4 \pi^4}{m^4 \pi^4 - \beta^4}\right) m\pi \sin \frac{m\pi L_1}{L}, \\
\text{CTC}_{36} &= -2 \sum_{m=1}^{\infty} \frac{m^3 \pi^3}{m^4 \pi^4 - \beta^4} \sin \frac{m\pi L_1}{L}, \\
\text{CTC}_{37} &= 2 \sum_{m=1}^{\infty} (-1)^m \left(1 - \frac{m^4 \pi^4}{m^4 \pi^4 - \beta^4}\right) m\pi \sin \frac{m\pi L_1}{L}, \\
\text{CTC}_{38} &= 2 \sum_{m=1}^{\infty} \frac{(-1)^m m^3 \pi^3}{m^4 \pi^4 - \beta^4} \sin \frac{m\pi L_1}{L}, \\
\text{CTC}_{41} &= 2 \sum_{m=1}^{\infty} \left(\left(1 - \frac{m^4 \pi^4}{m^4 \pi^4 - \beta^4}\right) m^2 \pi^2 \cos \frac{m\pi L_1}{L} - \bar{T}_a \frac{m^3 \pi^3}{m^4 \pi^4 - \beta^4} \sin \frac{m\pi L_1}{L} \right), \\
\text{CTC}_{42} &= - \left(1 + 2 \sum_{m=1}^{\infty} \left(\left(1 - \frac{m^4 \pi^4}{m^4 \pi^4 - \beta^4}\right) \cos \frac{m\pi L_1}{L} - \bar{T}_a \frac{m\pi}{m^4 \pi^4 - \beta^4} \sin \frac{m\pi L_1}{L} \right) \right), \\
\text{CTC}_{43} &= -2 \sum_{m=1}^{\infty} \left(\left(1 - \frac{m^4 \pi^4}{m^4 \pi^4 - \beta^4}\right) (-1)^m m^2 \pi^2 \cos \frac{m\pi L_1}{L} - \bar{T}_a \frac{(-1)^m m^3 \pi^3}{m^4 \pi^4 - \beta^4} \sin \frac{m\pi L_1}{L} \right), \\
\text{CTC}_{44} &= \left(1 + 2 \sum_{m=1}^{\infty} \left(\left(1 - \frac{m^4 \pi^4}{m^4 \pi^4 - \beta^4}\right) (-1)^4 \cos \frac{m\pi L_1}{L} - \bar{T}_a \frac{(-1)^m m\pi}{m^4 \pi^4 - \beta^4} \sin \frac{m\pi L_1}{L} \right) \right),
\end{aligned}$$

$$\text{CTC}_{45} = -2 \sum_{m=1}^{\infty} \left(1 - \frac{m^4 \pi^4}{m^4 \pi^4 - \beta^4} \right) m^2 \pi^2 \cos \frac{m\pi L_1}{L},$$

$$\text{CTC}_{46} = 1 + 2 \sum_{m=1}^{\infty} \left(1 - \frac{m^4 \pi^4}{m^4 \pi^4 - \beta^4} \right) \cos \frac{m\pi L_1}{L},$$

$$\text{CTC}_{47} = 2 \sum_{m=1}^{\infty} \left(1 - \frac{m^4 \pi^4}{m^4 \pi^4 - \beta^4} \right) (-1)^m m^2 \pi^2 \cos \frac{m\pi L_1}{L},$$

$$\text{CTC}_{48} = - \left(1 + 2 \sum_{m=1}^{\infty} \left(1 - \frac{m^4 \pi^4}{m^4 \pi^4 - \beta^4} \right) (-1)^m \cos \frac{m\pi L_1}{L} \right), \quad \text{CTC}_{51} = 1,$$

$$\text{CTC}_{52} = \text{CTC}_{53} = \text{CTC}_{54} = \text{CTC}_{55} = \text{CTC}_{56} = \text{CTC}_{57} = \text{CTC}_{58} = 0,$$

$$\text{CTC}_{61} = \text{CTC}_{62} = \text{CTC}_{63} = \text{CTC}_{64} = \text{CTC}_{65} = \text{CTC}_{66} = 0, \quad \text{CTC}_{67} = 1,$$

$$\text{CTC}_{88} = 0, \quad \text{CTC}_{71} = - \left(3 - 2 \sum_{m=1}^{\infty} \frac{m^4 \pi^4}{m^4 \pi^4 - \beta^4} \right), \quad \text{CTC}_{72} = -2 \sum_{m=1}^{\infty} \frac{m^2 \pi^2}{m^4 \pi^4 - \beta^4},$$

$$\text{CTC}_{73} = 1 + 2 \sum_{m=1}^{\infty} \left(1 - \frac{m^4 \pi^4}{m^4 \pi^4 - \beta^4} \right) (-1)^m, \quad \text{CTC}_{74} = 2 \sum_{m=1}^{\infty} \frac{m^2 \pi^2}{m^4 \pi^4 - \beta^4} (-1)^m,$$

$$\text{CTC}_{75} = \text{CTC}_{76} = \text{CTC}_{77} = \text{CTC}_{78} = 0, \quad \text{CTC}_{81} = \text{CTC}_{82} = \text{CTC}_{83} = \text{CTC}_{84} = 0,$$

$$\text{CTC}_{85} = - \left(1 + 2 \sum_{m=1}^{\infty} \left(1 - \frac{m^4 \pi^4}{m^4 \pi^4 - \beta^4} \right) (-1)^m \right),$$

$$\text{CTC}_{86} = -2 \sum_{m=1}^{\infty} \frac{(-1)^m m^2 \pi^2}{m^4 \pi^4 - \beta^4}, \quad \text{CTC}_{87} = \left(3 - 2 \sum_{m=1}^{\infty} \frac{m^4 \pi^4}{m^4 \pi^4 - \beta^4} \right),$$

$$\text{CTC}_{88} = 2 \sum_{m=1}^{\infty} \frac{m^2 \pi^2}{m^4 \pi^4 - \beta^4}.$$

References

- [1] R. Grief, S.C. Mittendorf, Structural vibrations and Fourier series, *Journal of Sound and Vibration* 48 (1) (1976) 113–122.
- [2] S.C. Mittendorf, R. Grief, Vibrations of segmented beams by a Fourier series component mode method, *Journal of Sound and Vibration* 55 (3) (1977) 431–441.
- [3] H. Chung, Analysis method for calculating vibration characteristics of beams with intermediate supports, *Nuclear Engineering and Design* 63 (1981) 55–80.
- [4] J.T.S. Wang, C.C. Lin, Dynamic analysis of generally supported beams using Fourier series, *Journal of Sound and Vibration* 196 (3) (1996) 285–293.
- [5] Natural frequencies of UCN5&6 fuel rod span length vs. excitation frequencies, KNFC Design Note No. U561CD-FA1-CN-023, Rev.0.
- [6] M.J. Maurizi, D.V. Bambil De Rossit, Free vibration of a clamped–clamped beam with an intermediate elastic support, *Journal of Sound and Vibration* 119 (1987) 173–176.
- [7] A.H. Register, A note on vibrations of generally restrained, end-loaded beams, *Journal of Sound and Vibration* 172 (1994) 561–571.
- [8] D.J. Gorman, *Free Vibration Analysis of Beams and Shafts*, Wiley, New York, 1975.
- [9] H.K. Kim, M.S. Kim, Vibration of beams with generally restrained boundary conditions using Fourier series, *Journal of Sound and Vibration* 245 (5) (2001) 771–784.